

Rational design of CYP3A4 inhibitors: A one-atom linker elongation in ritonavir-like compounds leads to a marked improvement in the binding strength

Eric R. Samuels^{†f} and Irina F. Sevrioukova^{‡*}

Departments of [†]Pharmaceutical Sciences and [‡]Molecular Biology and Biochemistry, University of California, Irvine, California 92697-3900

SUPPLEMENTAL MATERIALS

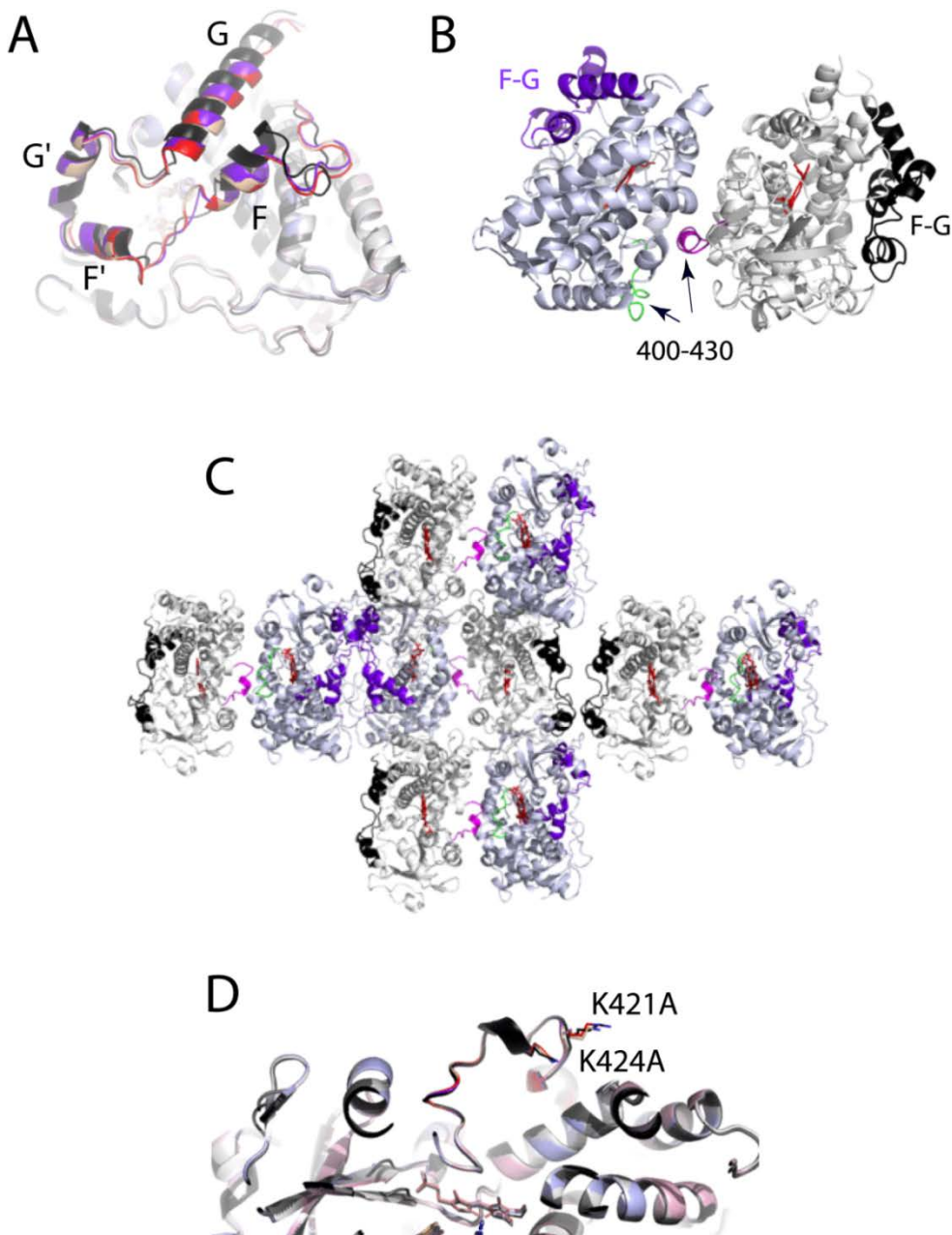


Figure S1. **(A)** Restructuring of the F-F' helix/loop region triggered by distinct crystal packing in the C2 space group. The F-F'-G'-G fragments of ligand-free (5VCE; I222) and **3a-**, **3e-** and **3i**-bound CYP3A4 (C2) are shown in black, red, beige and purple, respectively. **(B, C)** Crystallographic dimer of CYP3A4 and its spatial arrangement in C2 crystals, respectively. The 400-430 fragment (in green and magenta) is at the monomer-monomer interface, whereas the F-G fragment (in black and purple) mediates inter-dimer contacts. **(D)** A view at the proximal face of CYP3A4. The water-bound protein (5VCC structure) is in gray; **3a-** and **3e**-bound complexes of WT CYP3A4 are in pink and light blue, respectively; and **3i**-bound K421A/K424A CYP3A4 is in black. Structural superposition shows that substitution of surface K421 and K424 with alanine does not distort the proximal loop region. Non-mutated lysine side chains are displayed.

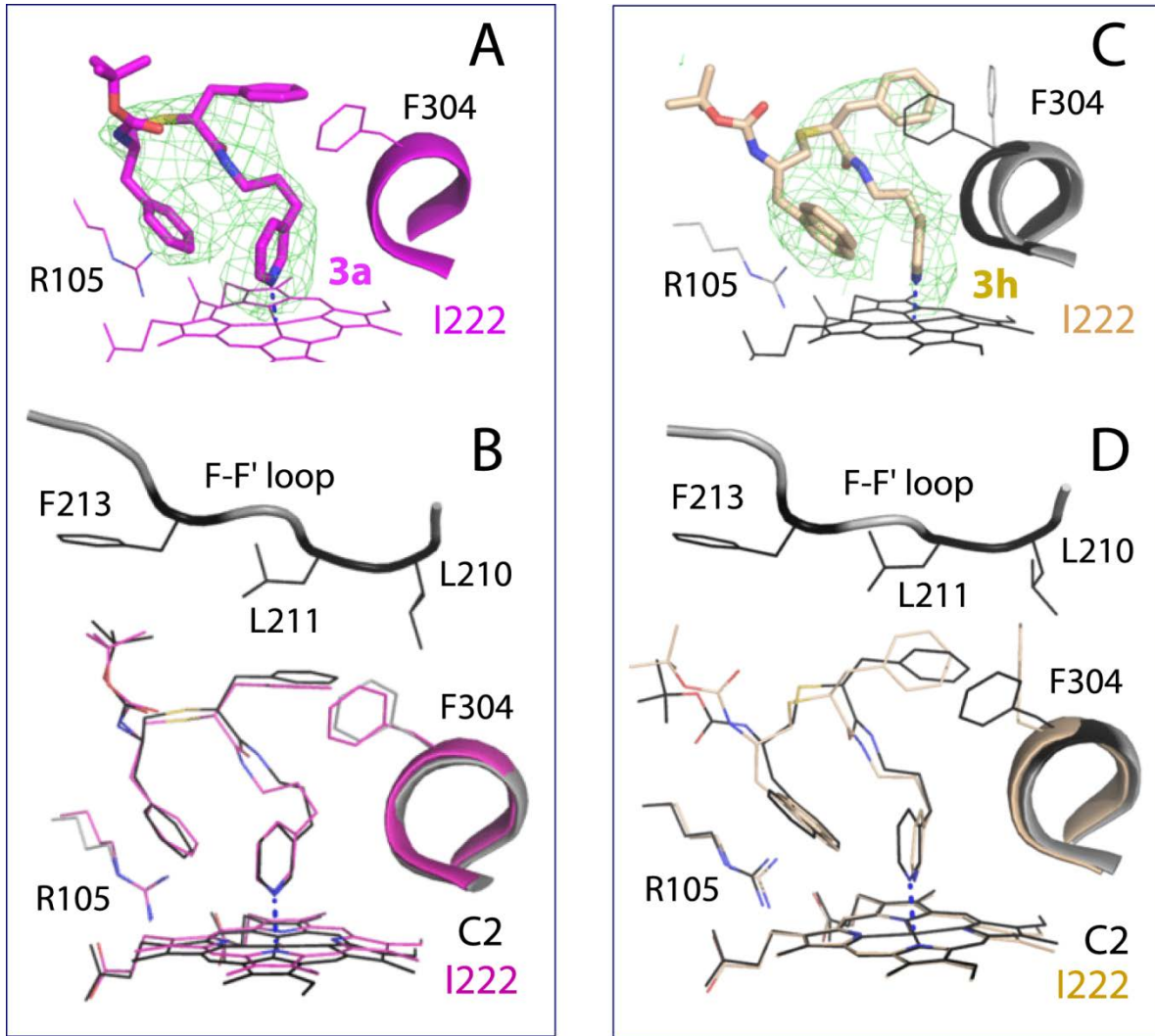


Figure S2. Binding of **3a** (**A**, **B**) and **3h** (**B**, **C**) to the active site of CYP3A4 crystallized in I222 and C2 space groups. For both **3a** and **3h**, electron density maps were not clearly defined in the I222 structures (green mesh in **A** and **C**, respectively). Therefore, **3a**- and **3h**-bound CYP3A4 was recrystallized in a more densely packed C2 space group. (**B**, **D**) Comparison of the ligand binding modes observed in the I222 and C2 structures shows that there are virtually no (for **3a**) or only minor distortions (for **3h**), primarily imposed by changes in the F-F' loop (residues 210-213).

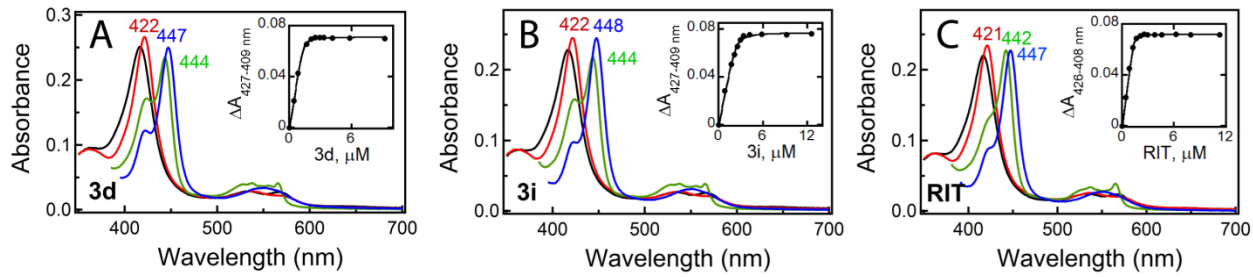


Figure S3. Spectral and ligand-binding properties of K421A/K424A CYP3A4. **(A-C)** Spectral changes induced in the mutant by **3d**, **3i** and ritonavir, respectively. Absorbance spectra of ferric ligand-free and inhibitor-bound CYP3A4 (2 μM) were recorded in 0.1 M phosphate buffer, pH 7.4, supplemented with 20% glycerol and 1 mM dithiothreitol, and displayed in black and red, respectively. Spectra of the ferrous form and its CO-adduct are in green and blue, respectively. The inhibitor concentration was 10 μM. Equilibrium titrations were conducted as described in the Materials and Methods section in the main text. Titration plots with quadratic fittings are shown in insets. The derived dissociation constants were 0.019 μM, 0.025 μM and 0.023 μM for **3d**, **3i** and ritonavir, respectively.

Table S1. Data collection and refinement statistics

Ligand	3a	3b	3c	3d	8
CYP3A4	WT	WT	WT	K421A/K424A	WT
PDB ID	7KNH	7KVI	7KVJ	7VKV	7KVM
Data statistics					
Space group	C2	I222	I222	C2	I222
Unit cell	$a, b, c = 93 \times 95 \times 153 \text{ \AA}$; $\alpha, \beta, \gamma = 90^\circ \times 90^\circ \times 124^\circ$	$a, b, c = 77 \times 103 \times 126 \text{ \AA}$; $\alpha, \beta, \gamma = 90^\circ$	$a, b, c = 76 \times 100 \times 124 \text{ \AA}$; $\alpha, \beta, \gamma = 90^\circ$	$a, b, c = 76 \times 101 \times 125 \text{ \AA}$; $\alpha, \beta, \gamma = 90^\circ$	$a, b, c = 78 \times 101 \times 129 \text{ \AA}$; $\alpha, \beta, \gamma = 90^\circ$
Resolution range (\AA)	39.55-2.79 (2.79-2.94) ^a	79.64-2.55 (2.55-2.69)	78.17-2.65 (2.79-2.65)	77.80-2.55 (2.69-2.55)	79.64-2.70 (2.85-2.70)
Total reflections	167,933	81,756	51,716	159,292	56,723
Unique reflections	27,176	16,474	13,659	37,311	13,668
Redundancy	6.2 (6.0)	5.0 (4.8)	3.8 (4.0)	4.3 (4.4)	4.2 (4.3)
Completeness	98.3 (96.9)	99.2 (99.5)	97.1 (98.3)	99.8 (99.8)	95.9 (97.4)
Average $\text{I}/\sigma\text{I}$	5.8 (1.1)	8.3 (1.0)	7.4 (1.0)	8.4 (1.1)	8.5 (0.9)
R_{merge}	0.163 (2.561)	0.077 (1.163)	0.070 (2.029)	0.080 (1.443)	0.047 (2.926)
R_{pim}	0.107 (1.155)	0.038 (0.592)	0.042 (1.127)	0.043 (0.768)	0.038 (1.358)
CC ½	0.993 (0.489)	0.998 (0.532)	0.998 (0.320)	0.999 (0.398)	0.996 (0.313)
Refinement statistics					
R/R_{free}^b	23.8/27.8	22.5/26.2	22.5/28.0	23.7/27.7	22.7/27.6
Number of atoms:					
Protein	3657/3555 ^c	3654	3341	3716/3581	3720
Solvent	24	21	4	14	0
R.m.s. deviations					
Bond lengths, \AA	0.002	0.002	0.002	0.002	0.003
Bond angles, $^\circ$	0.490	0.531	0.490	0.467	0.661
Wilson B-factor, \AA^2	83	79	96	73	112
Average B -factor, \AA^2 :					
Protein	91/110 ^c	112	136	89/131	141
Ligand	85/104 ^c	140	162	102/126	149
Ramachandran plot ^d (residues; %)					
Preferred	816 (93.0%)	427 (96.0%)	388 (95.0%)	848 (94.9%)	435 (95.0%)
Allowed	60 (6.8%)	17 (3.8%)	20 (5.0%)	44 (4.9%)	25 (5.0%)
Outliers	2 (0.2%)	1 (0.2%)	none	2 (0.2%)	none

^aValues in brackets are for the highest resolution shell.^b R_{free} was calculated from a subset of 5% of the data that were excluded during refinement.^cValues for two molecules in the asymmetric unit.^dAnalyzed with PROCHECK.

Table S2. Data collection and refinement statistics

Ligand	3e	3f	3g	3h	3i
CYP3A4	WT	WT	WT	WT	K421A/K424A
PDB ID	7KVN	7KVO	7KVP	7KVQ	7KVS
<i>Data statistics</i>					
Space group	C2	I2	I222	C2	C2
Unit cell	$a, b, c = 93 \times 96 \times 153 \text{ \AA}$; $\alpha, \beta, \gamma = 90 \times 90 \times 124^\circ$	$a, b, c = 93 \times 98 \times 128 \text{ \AA}$; $\alpha, \beta, \gamma = 90 \times 90 \times 93^\circ$	$a, b, c = 78 \times 102 \times 128 \text{ \AA}$; $\alpha, \beta, \gamma = 90^\circ$	$a, b, c = 93 \times 97 \times 154 \text{ \AA}$; $\alpha, \beta, \gamma = 90 \times 90 \times 124^\circ$	$a, b, c = 93 \times 98 \times 155 \text{ \AA}$; $\alpha, \beta, \gamma = 90 \times 90 \times 124^\circ$
Resolution range (Å)	76.93-2.70 (2.85-2.70) ^a	49.04-2.65 (2.79-2.65)	80.00-2.75 (2.907-2.75)	77.28-2.70 (2.85-2.70)	77.82-2.50 (2.64-2.50)
Total reflections	136,528	223,503	43,178	177,490	246,329
Unique reflections	28,152	33,059	13,250	30,116	38,953
Redundancy	4.8 (4.3)	6.8 (6.7)	3.3 (3.4)	5.9 (6.0)	6.3 (6.3)
Completeness	91.9 (84.0)	99.9 (99.9)	97.3 (98.6)	94.4 (97.2)	97.6 (97.4)
Average $\ /\sigma\ $	4.0 (1.0)	12.3 (1.1)	5.9 (0.7)	8.5 (1.1)	11.0 (1.0)
R_{merge}	0.233 (1.598)	0.070 (2.278)	0.072 (2.466)	0.093 (1.641)	0.075 (1.922)
R_{pim}	0.115 (0.841)	0.029 (0.944)	0.045 (1.566)	0.040 (0.723)	0.032 (0.830)
CC $\frac{1}{2}$	0.970 (0.571)	0.999 (0.390)	0.998 (0.481)	0.999 (0.372)	0.999 (0.345)
<i>Refinement statistics</i>					
$R/R_{\text{free}}^{\text{b}}$	24.8/29.0	24.1/29.3	22.7/27.3	25.0/28.0	23.5/27.5
Number of atoms:					
Protein	3653/3646 ^c	3721/3631	3653	3669/3605	3689/3538
Solvent	88	0	2	0	47
R.m.s. deviations					
Bond lengths, Å	0.003	0.003	0.004	0.002	0.002
Bond angles, °	0.563	0.570	0.731	0.497	0.500
Wilson B-factor, Å ²	69	91	113	89	80
Average B-factor, Å ² :					
Protein	75/93 ^c	107/160	96	100/167	99/151
Ligand	65/88 ^c	164/177	163	128/177	132/182
Ramachandran plot ^d (residues; %)					
Preferred	826 (92.9%)	842 (94.1%)	435 (97.0%)	837 (93.9%)	836 (94.1%)
Allowed	62 (9.0%)	52 (5.8%)	14 (3.0%)	53 (6.0%)	51 (5.8%)
Outliers	1 (0.1%)	1 (0.1%)	none	1 (0.1%)	1 (0.1%)

^aValues in brackets are for the highest resolution shell.^b R_{free} was calculated from a subset of 5% of the data that were excluded during refinement.^cValues for two molecules in the asymmetric unit.^dAnalyzed with PROCHECK

Table S3. Local correlation coefficients (CC) and CC_{peak} between three polder maps ($F_{\text{obs}} = |F_{\text{model}}|$)

Map 1 (m1), calculated F_{obs} assuming that the omitted ligand atoms are present. Map 2 (m2), calculated F_{obs} assuming that the omitted ligand atoms are not present. Map 3 (m3), polder map using experimental data.

Ligand/PDB ID	m1-m2		m1-m3		m2-m3	
	CC	CC _{peak}	CC	CC _{peak}	CC	CC _{peak}
3a 7K VH	0.4949	0.4797	0.8790	0.8579	0.4998	0.4709
3b 7K VI	0.6654	0.6106	0.8934	0.8439	0.6464	0.6431
3c 7K NJ	0.6304	0.6167	0.8333	0.7082	0.4517	0.3954
3d 7K V K	0.5390	0.4609	0.9078	0.8797	0.5149	0.4463
8 7K VM	0.6183	0.5721	0.8442	0.7824	0.6879	0.6878
3e 7K VN	0.5025	0.5048	0.8715	0.8431	0.4884	0.4780
3f 7K VO	0.7812	0.7598	0.8015	0.7899	0.6965	0.6741
3g 7K VP	0.6169	0.6394	0.8884	0.8461	0.5352	0.5618
3h 7K V Q	0.6701	0.6616	0.8005	0.7598	0.6414	0.6466
3i 7K VS	0.6324	0.6383	0.8551	0.8222	0.7047	0.6985

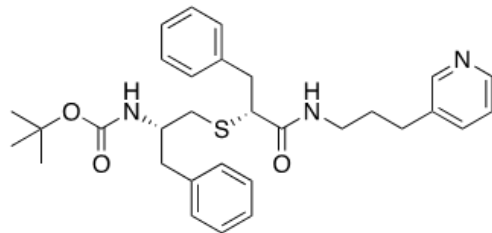
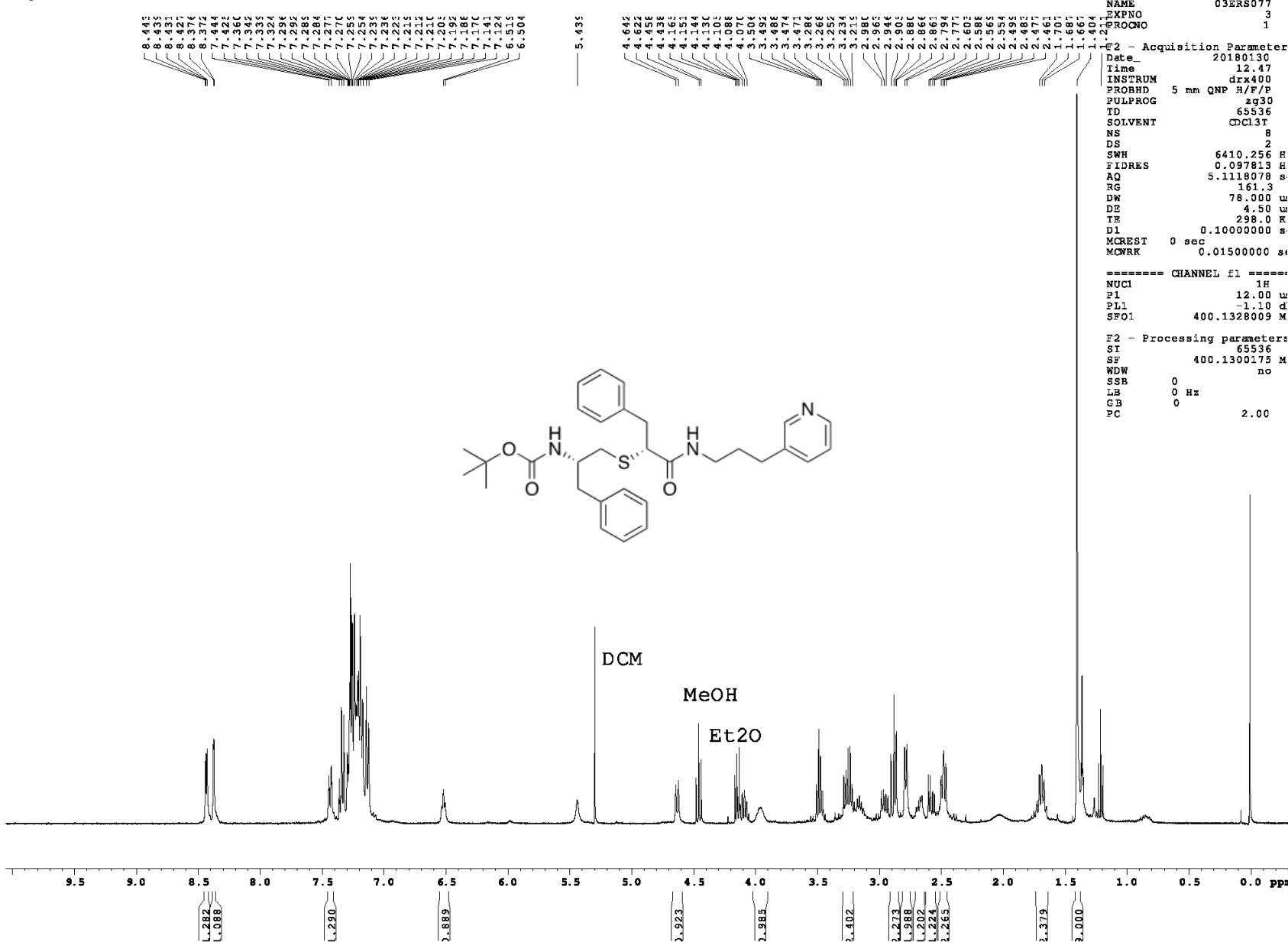
Correlation coefficients for polder maps were calculated using phenix.polder in the PHENIX software package.¹

For all ligands, CC(1,3) was > 0.8 and higher than CC(1,2) and CC(2,3), meaning that the polder maps displayed in Figures 3 and 6 of the main text show the omitted ligand atoms.²

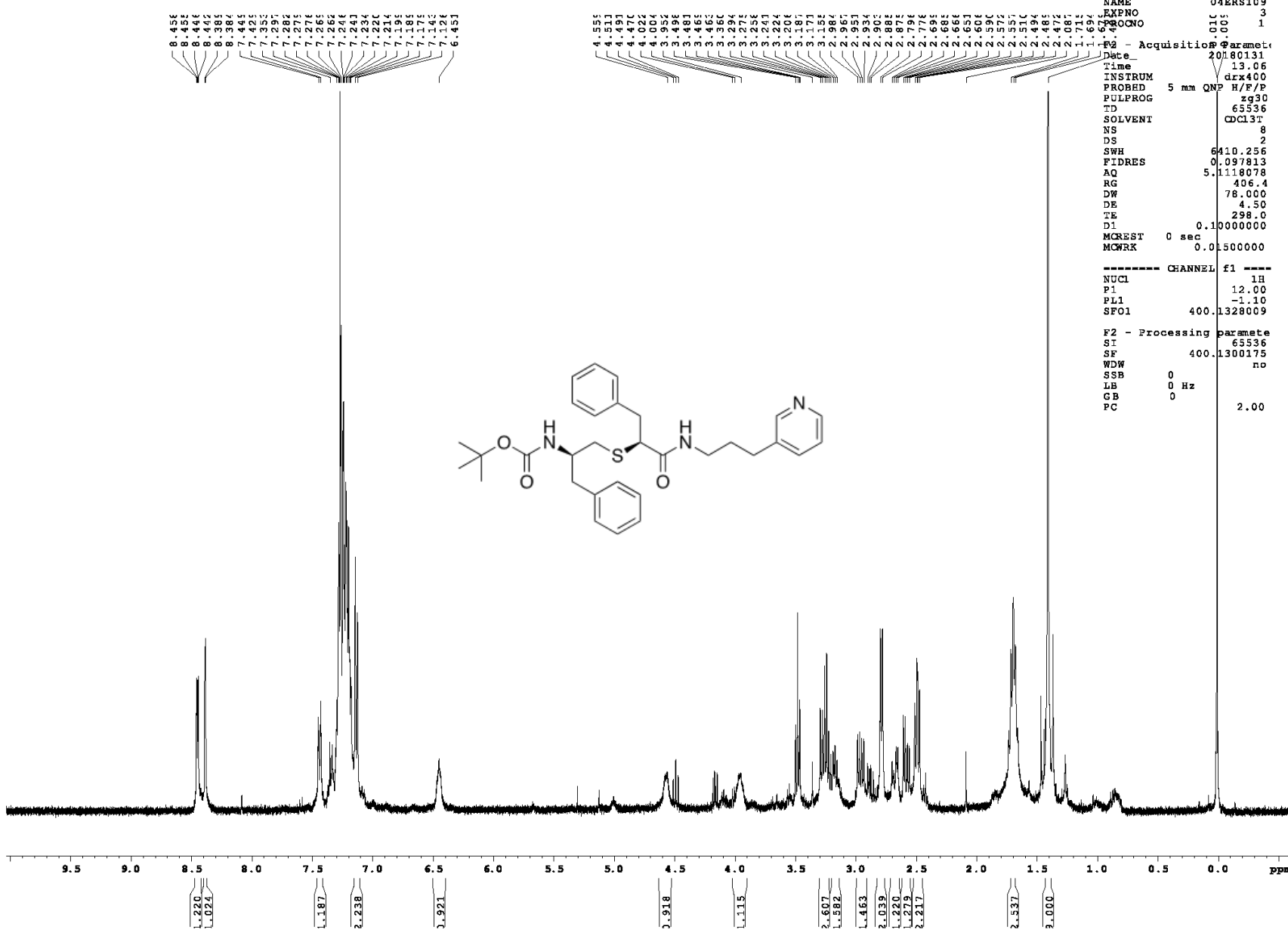
¹Adams, P.D.; Afonine, P.V.; Bunkoczi, G.; Chen, V.B.; Davis, I.W.; Echols, N.; Headd, J.J.; Hung, L.W.; Kapral, G.J.; Grosse-Kunstleve, R.W., et al. PHENIX: a comprehensive Python-based system for macromolecular structure solution. *Acta Crystallogr. Section D* **2010**, 66, 213-321

²Liebschner D., Afonine P.V.; Moriarty N.W.; Poon B.K.; Sobolev O.V.; Terwilliger T.C.; Adams P.D. Polder maps: improving OMIT maps by excluding bulk solvent. *Acta Crystallogr. Section D* **2016**, 73, 148-157.

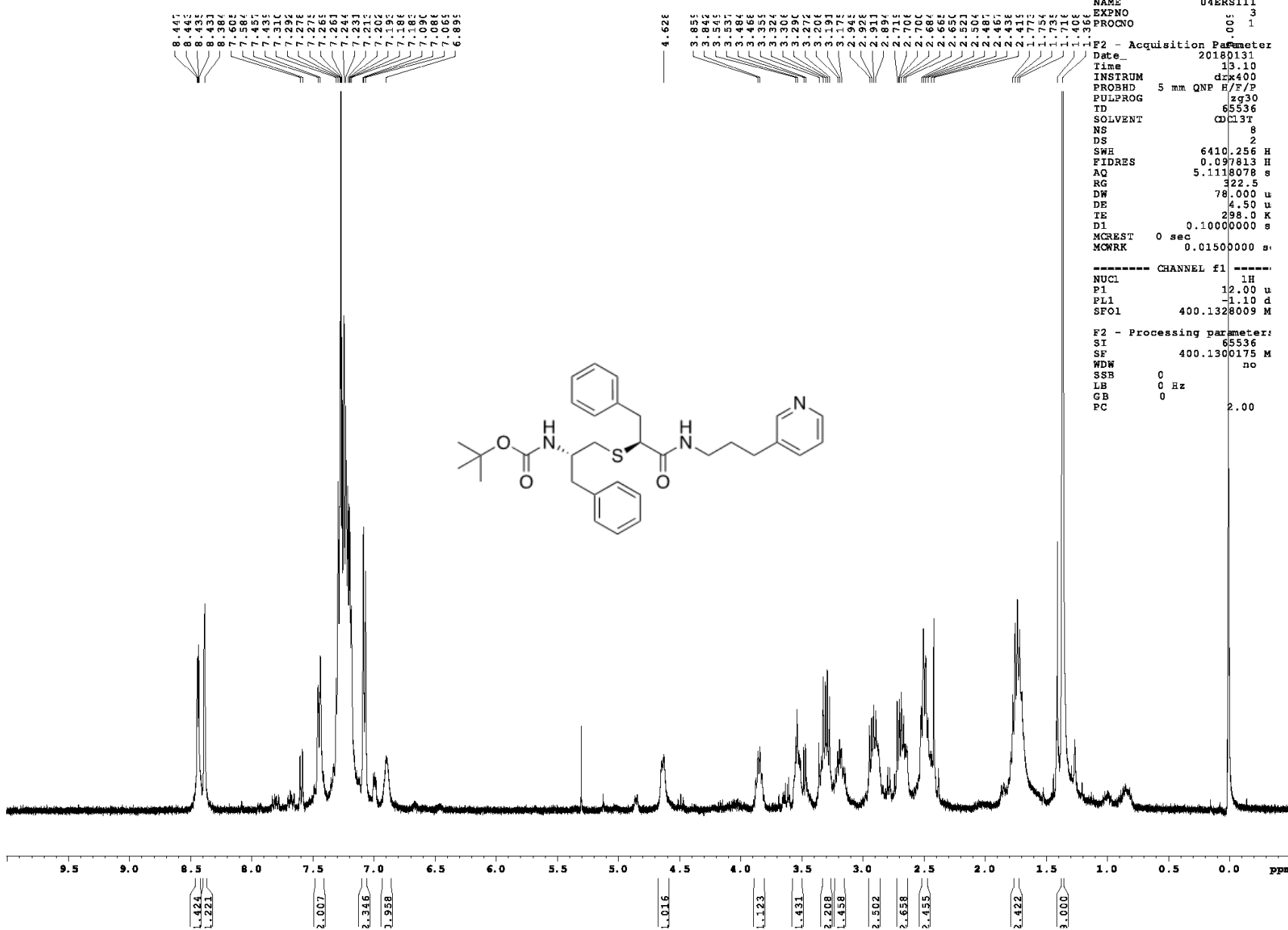
1H spectrum



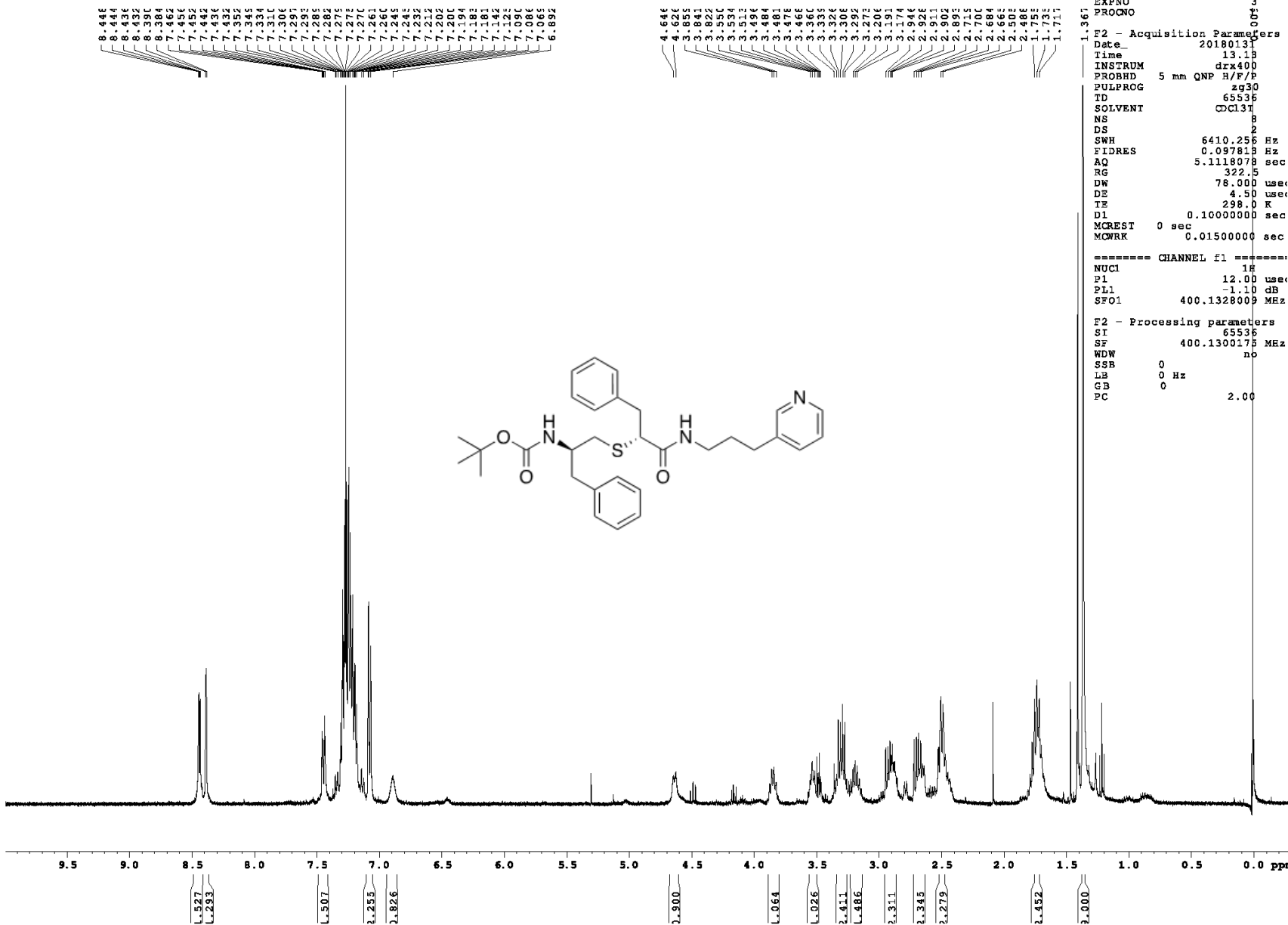
1H spectrum



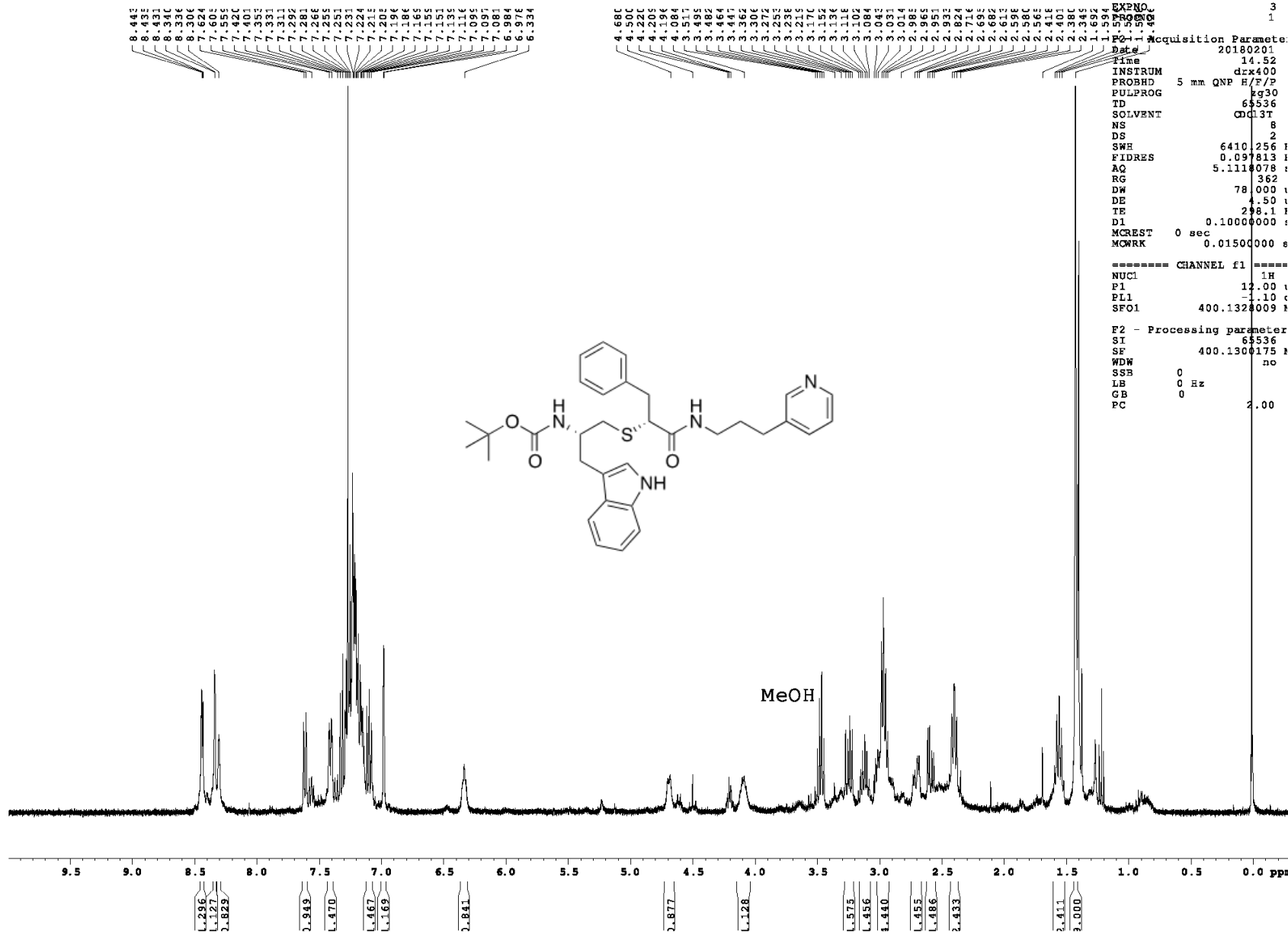
1H spectrum



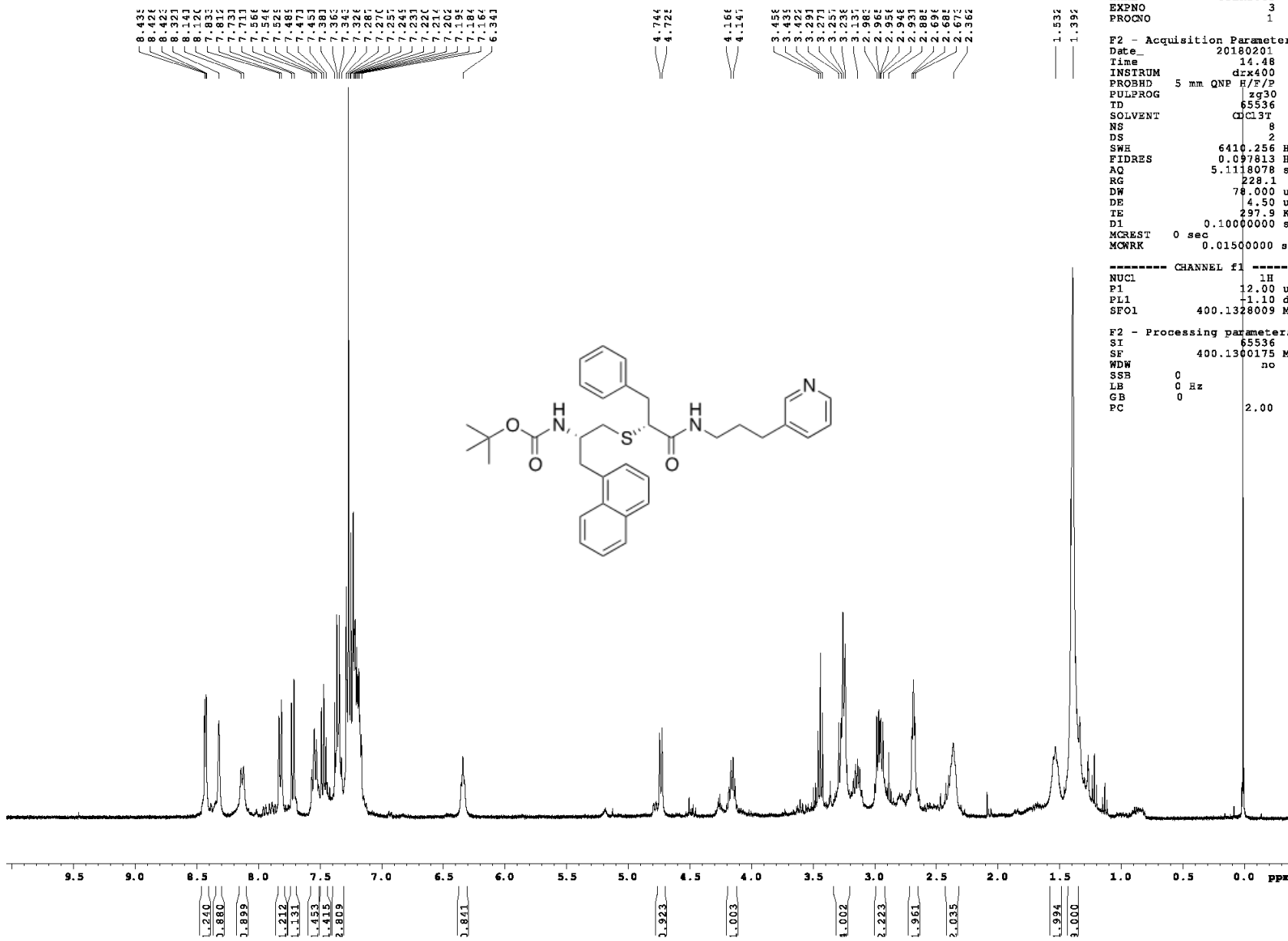
1H spectrum



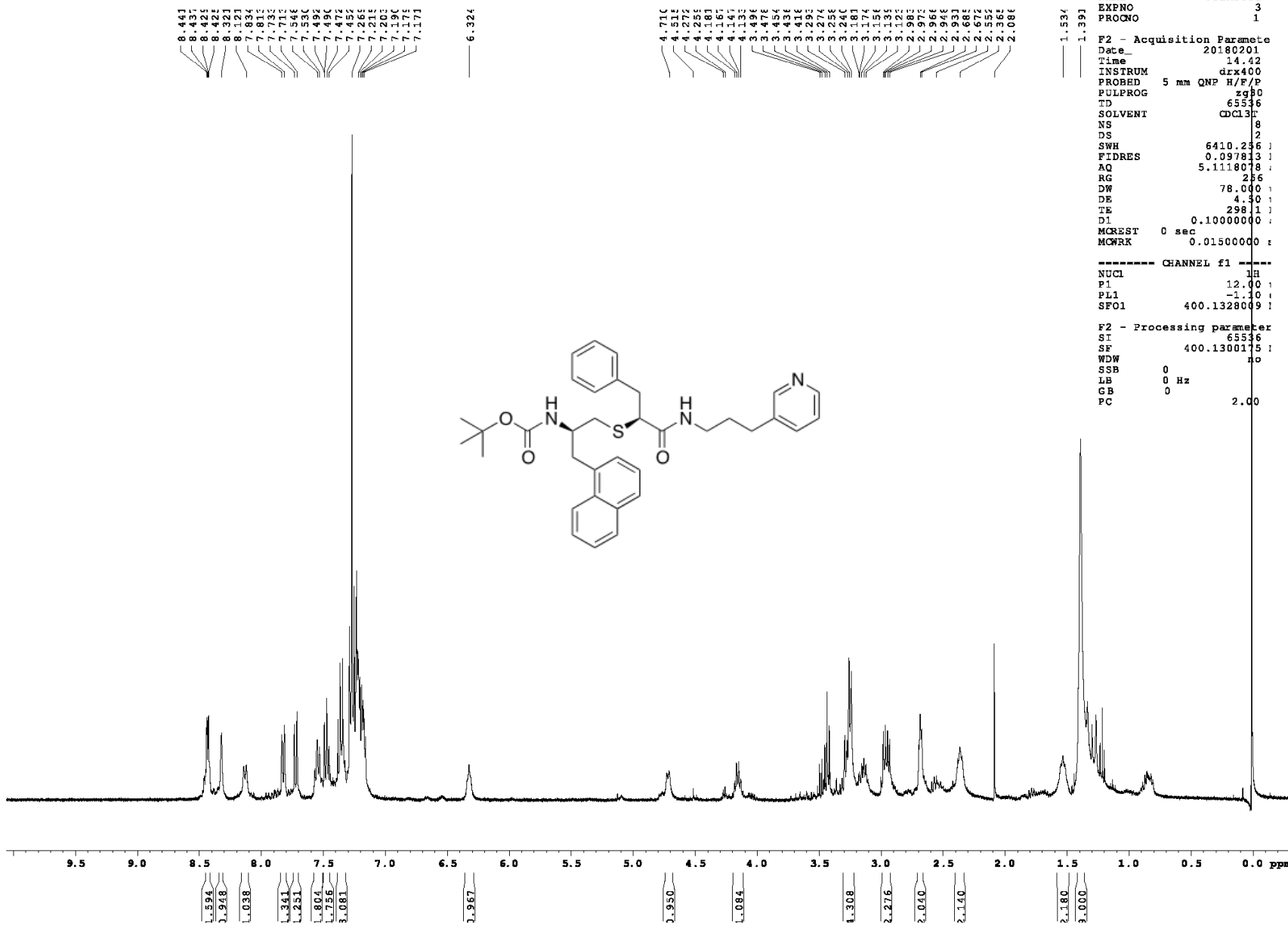
1H spectrum



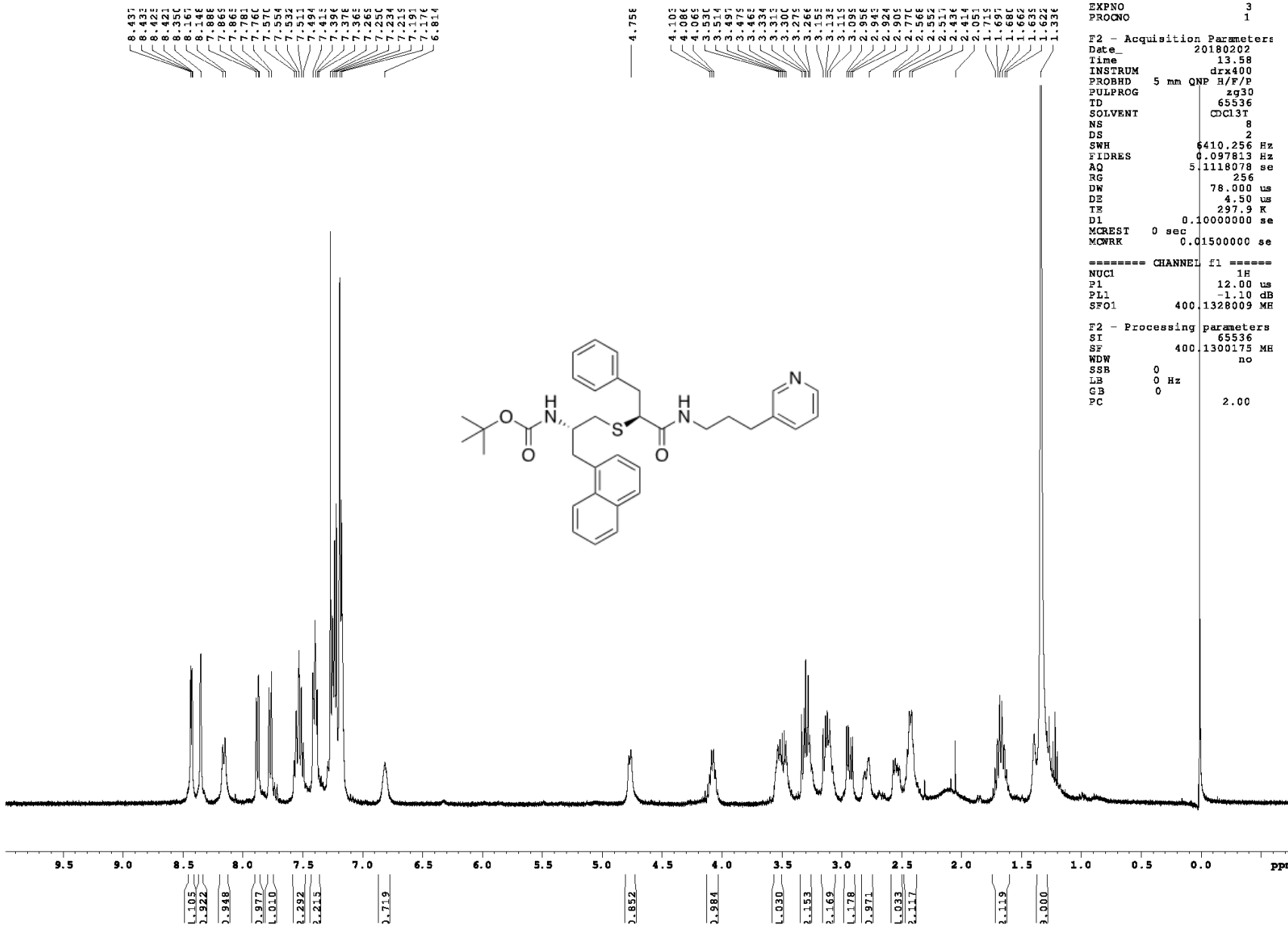
1H spectrum



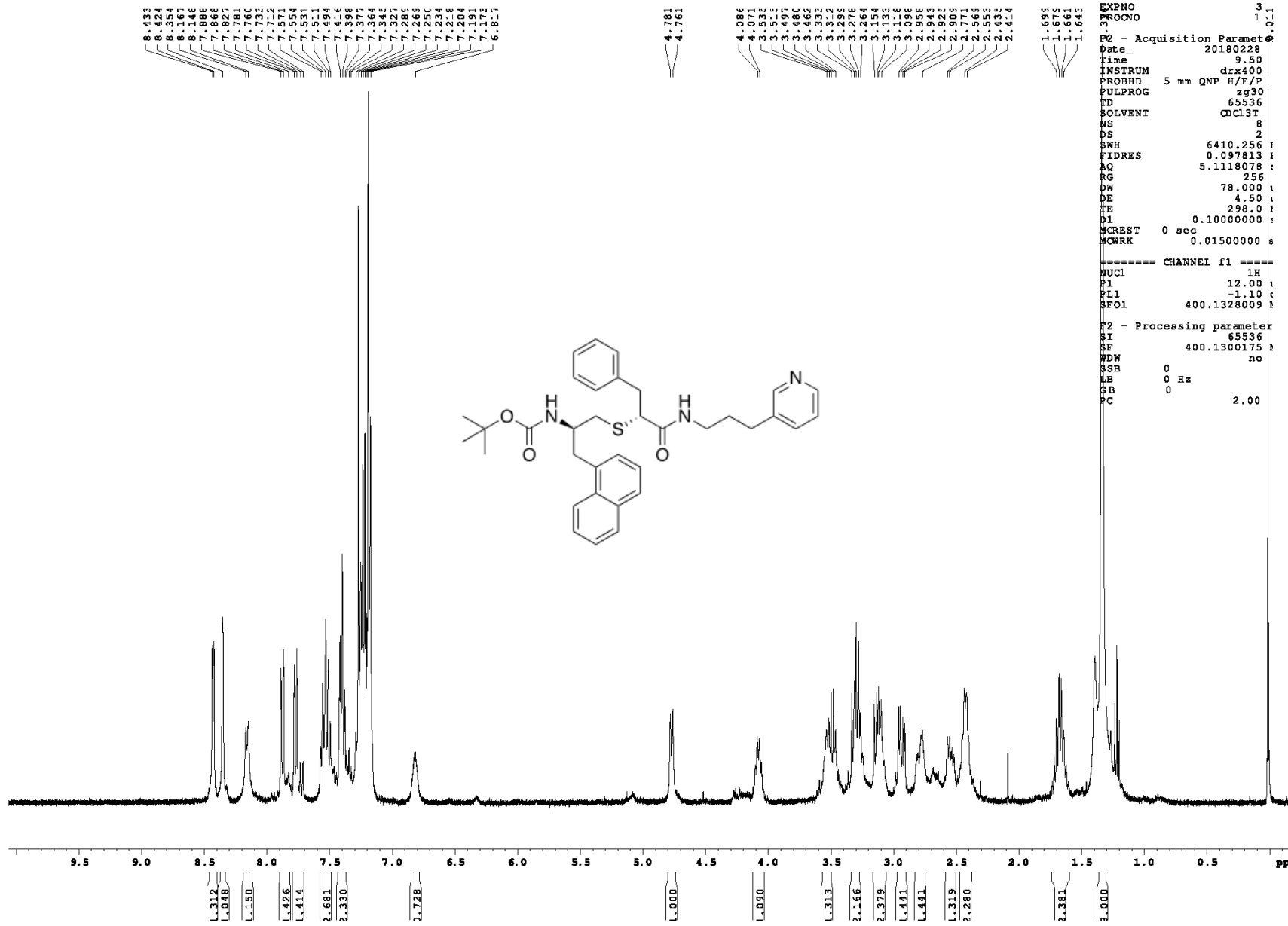
1H spectrum



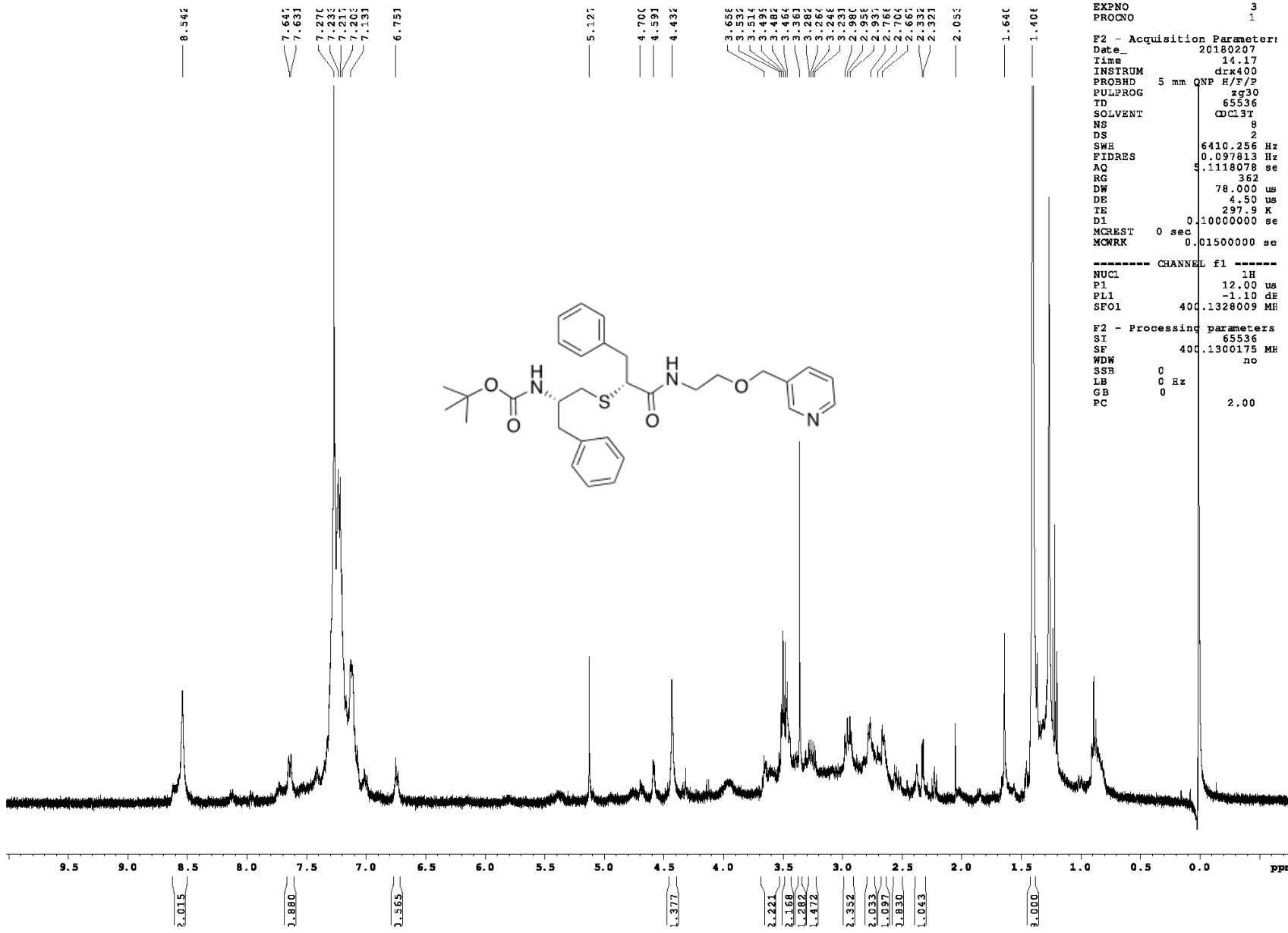
1H spectrum



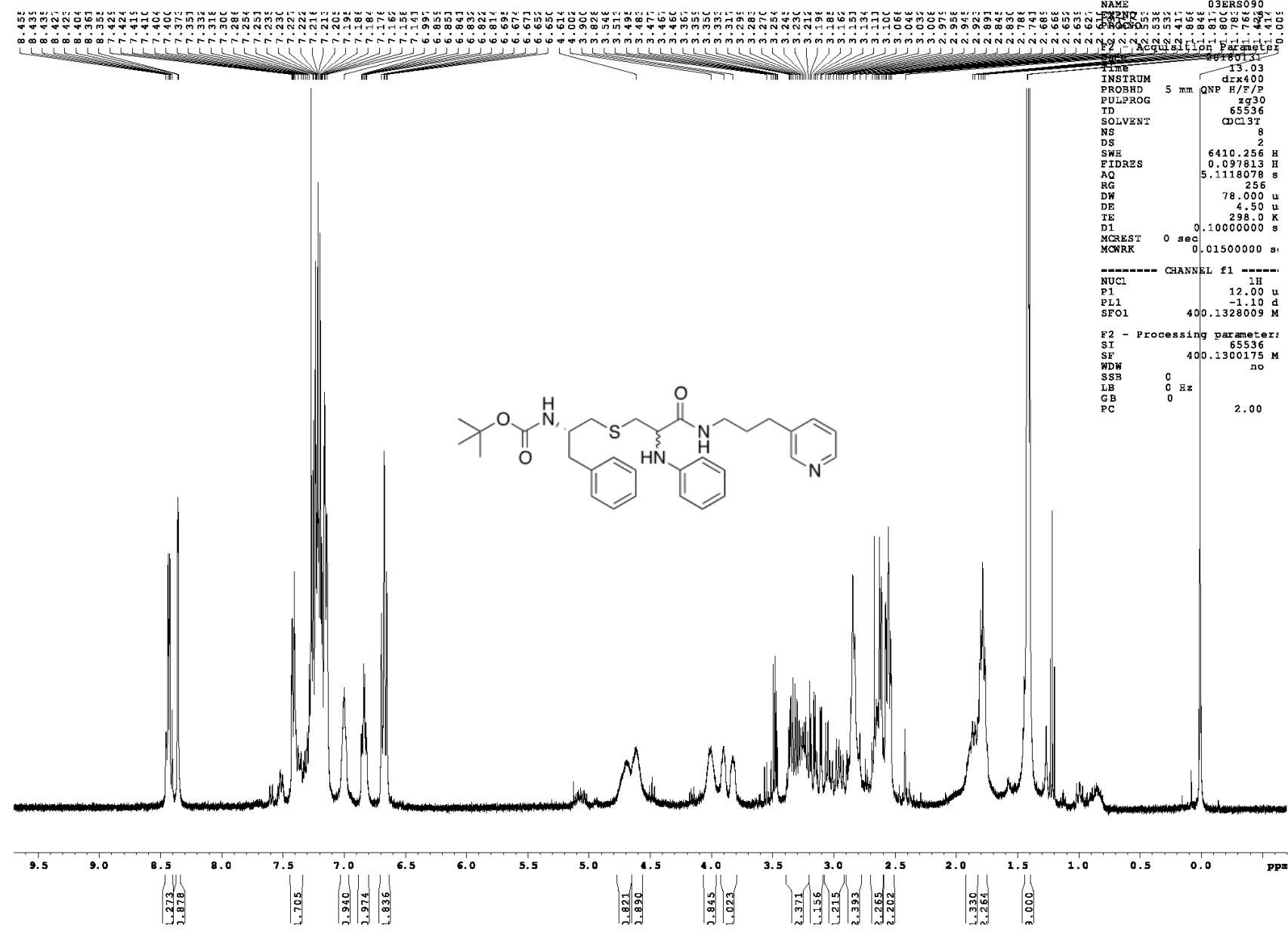
1H spectrum



1H spectrum

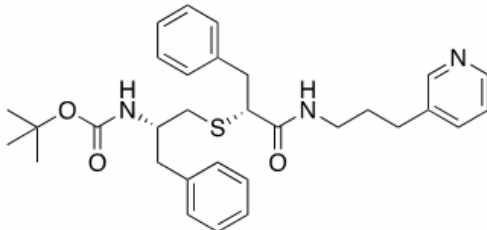
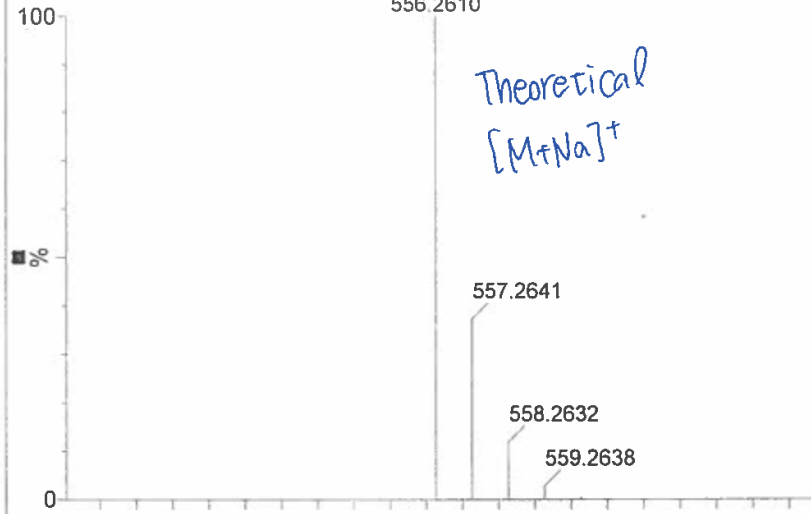


1H spectrum



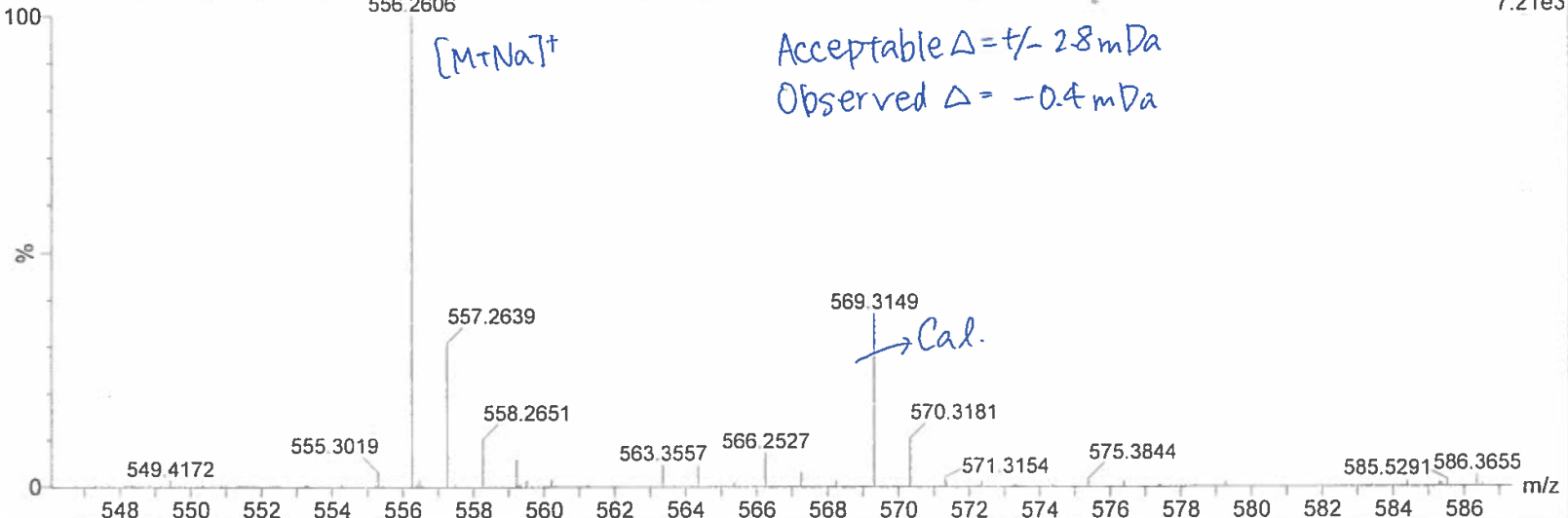
ES-377-a (0.019) ls (1.00,0.01) C₃₁H₃₉N₃O₃Na
556.2610

TOF MS ES+
6.58e12



ES-377-a 18 (0.330) AM (Cen,5, 80.00, Ar,8000.0,569.31,0.70); Sm (SG, 2x3.00); Sb (1,40.00)
556.2606

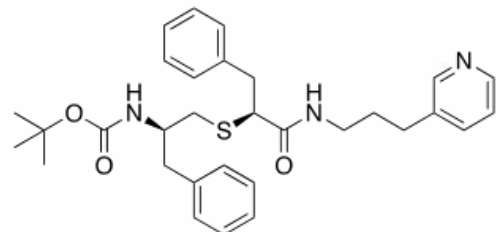
TOF MS ES+
7.21e3



4109_a (0.019) ls (1.00,0.01) C₃₁H₃₉N₃O₃Sn₄

100

%

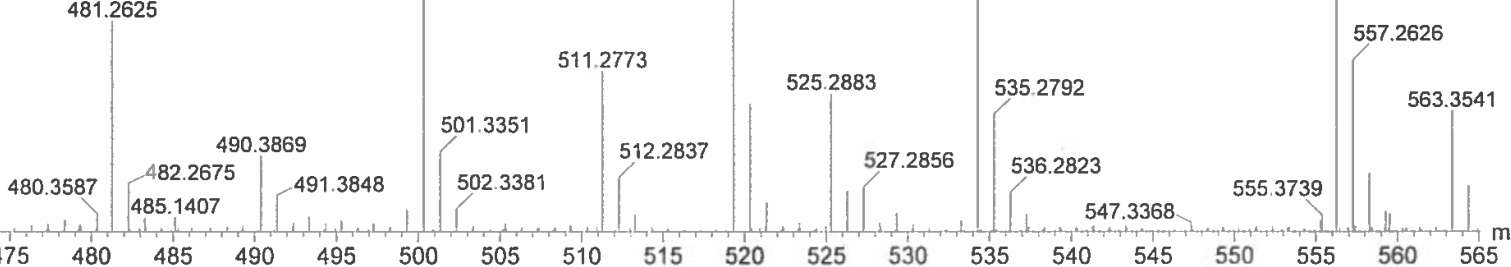


4109_a 20 (0.367) AM (Cen,5, 80.00, Ar,8000.0,481.26,0.70); Sm (SG, 2x3.00); Sb (1,40.00); Cm (17:31)

100

%

Cal



TOF MS ES+
6.58e12

Theoretical
 $[M+Na]^+$

556.2610

557.2641

558.2632

559.2638

TOF MS ES+
1.79e4

Acceptable = ± 3 mDa
Observed = - 2.3 mDa

Observed
 $[M+Na]^+$

556.2587

557.2626

563.3541

547.3368

555.3739

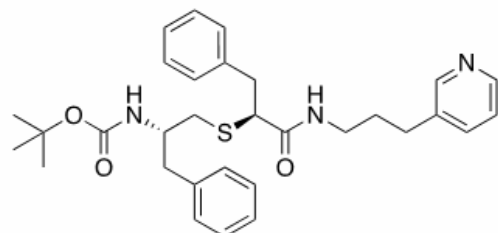
4111_a (0.019) ls (1.00,0.01) C₃₁H₃₉N₃O₃Sn₄

TOF MS ES+
6.58e12

100

%

0



556.2610

Theoretical
 $[M + Na]^+$

557.2641

558.2632

559.2638

4111_a 18 (0.330) AM (Cen,5, 80.00, Ar,8000.0,481.26,0.70); Sm (SG, 2x3.00); Sb (1,40.00); Cm (18:23)

TOF MS ES+
1.22e4

100

%

0

Acceptable = ± 3 mDa
Observed = -2.5 mDa

556.2585

→ Observed
 $[M + Na]^+$

481.2625

482.2696

500.3353

499.3154

519.3285

511.2712

502.3368

525.2888

534.2784

535.2819

536.2808

550.6259

557.2625

569.3157

570.3214

587.5464 600.3730

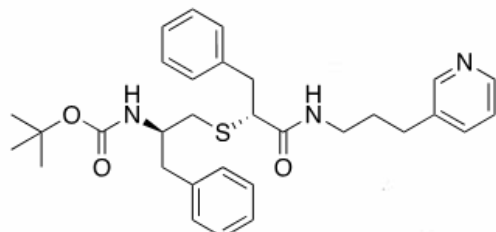
613.3443

m/z

4115_a (0.019) ls (1.00,0.01) C₃₁H₃₉N₃O₃Na

TOF MS ES+
6.58e12

100



556.2610

theoretical
[M+Na]⁺

557.2641

558.2632

559.2638

4115_a 29 (0.532) AM (Cen,5, 80.00, Ar,8000.0,525.29,0.70); Sm (SG, 2x3.00); Sb (1,40.00); Cm (29:39)

TOF MS ES+
7.95e3

100

500.3339

519.3288

Acceptable = ± 3 mDa
Observed = - 1.2 mDa

556.2598

[M+Na]⁺
observed

%

501.3365

511.2741

512.2806

525.2887

534.2791

526.2924

535.2824

536.2821

547.3530

555.3033

557.2641

569.3157

570.3323

584.3931

588.3860

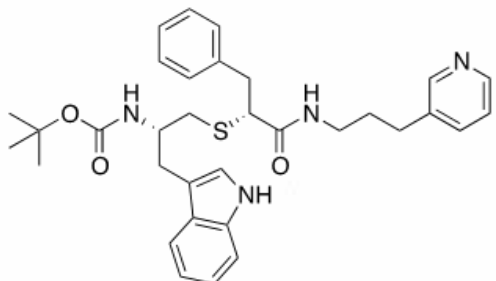
600.3831

m/z

397_a (0.019) ls (1.00,0.01) C33H41N4O3S

TOF MS ES+
6.41e12

100



573.2899

$(\text{M}+\text{H})^+$
Theoretical

574.2930

575.2924
576.2930

397_a 19 (0.349) AM (Cen,5, 80.00, Ar,8000.0,525.29,0.70); Sm (SG, 2x3.00); Sb (1,40.00); Cm (19.30)

TOF MS ES+
1.92e4

100

Acceptable = $\pm 3 \text{ mDa}$
Observed = $+0.1 \text{ mDa}$

Cal

519.3295

525.2887

511.2708

526.2917
527.2912

541.2946

555.2975

563.3563

569.3146

574.2928

575.3023

575.3771

587.5342

595.2708

596.2738

597.2756

598.2838

608.3811

0

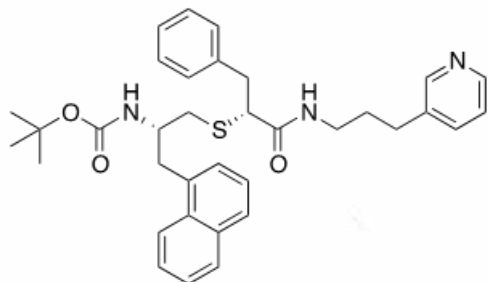
510 515 520 525 530 535 540 545 550 555 560 565 570 575 580 585 590 595 600 605

m/z

383_a (0.019) ls (1.00,0.01) C35H42N3O3S

TOF MS ES+
6.30e12

100



584.2947

(M+H)⁺
Theoretical

585.2979

586.2974

587.2980

383_a 22 (0.404) AM (Cen,5, 80.00, Ar,8000.0,525.29,0.70); Sm (SG, 2x3.00); Sb (1,40.00); Cm (22:34)

TOF MS ES+
2.03e4

100

Acceptable = ± 3 mDa
Observed = -2.6 mDa

Cal

525.2887

526.2936

534.2841 541.2755

556.2692

553.3563

569.3136

570.3234

585.2963

586.2997

587.3090

599.4719

606.2735

607.2795

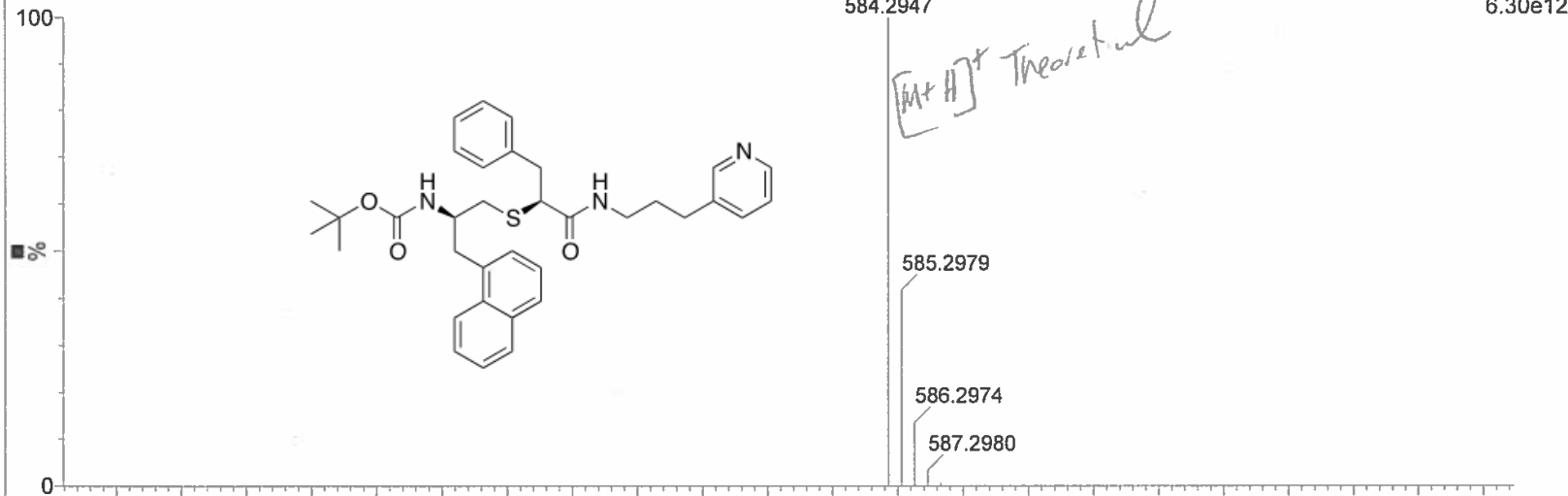
608.2820

619.4064

m/z

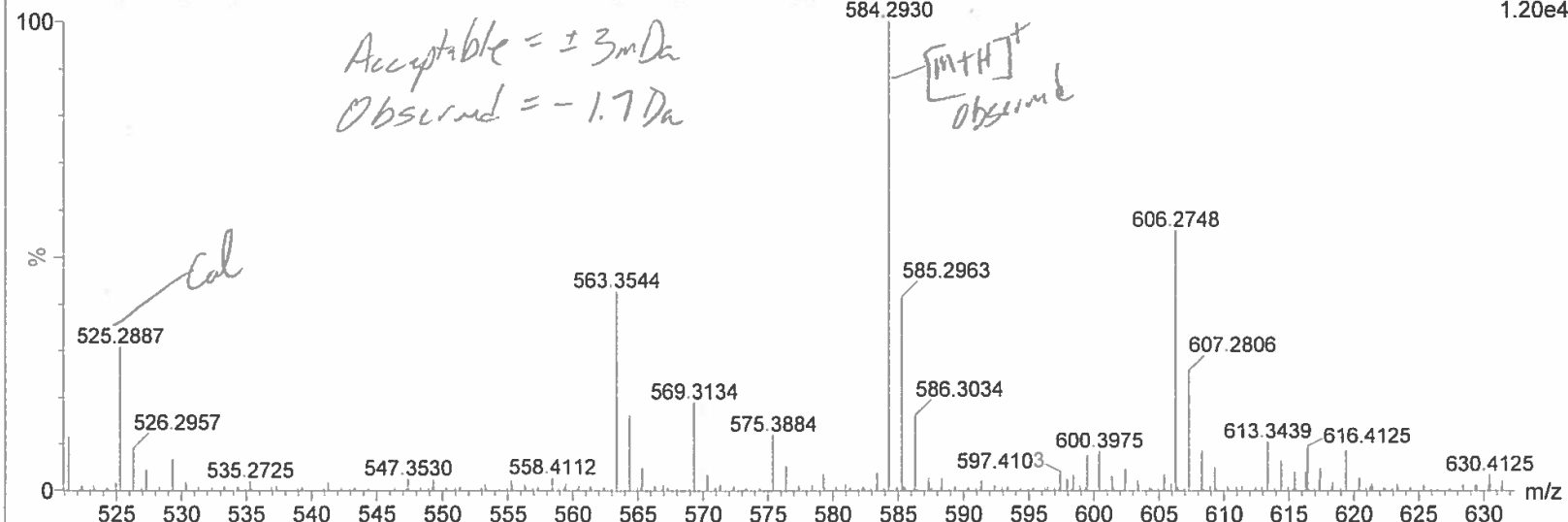
381_a (0.019) ls (1.00,0.01) C₃₅H₄₂N₃O₃S

TOF MS ES+
6.30e12



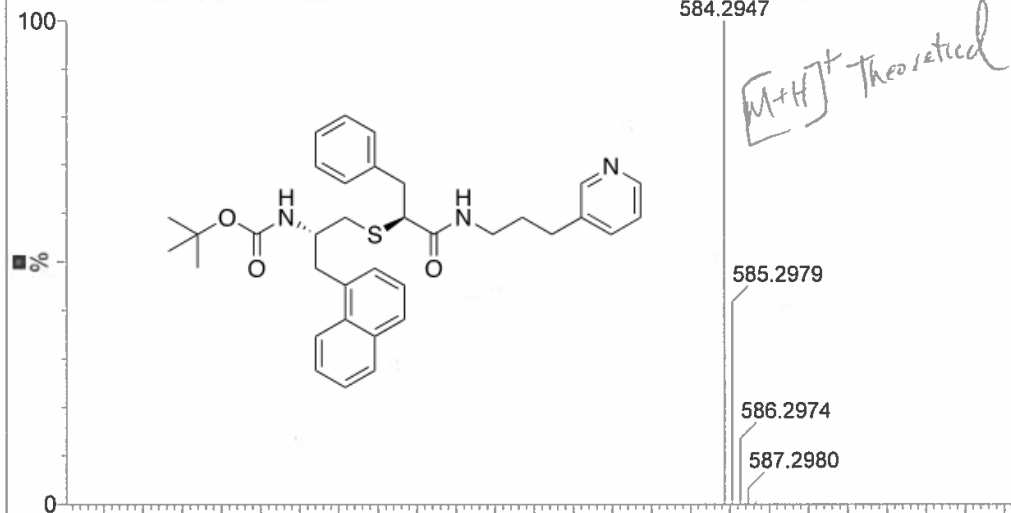
381_a 25 (0.458) AM (Cen,5, 80.00, Ar,8000.0,525.29,0.70); Sm (SG, 2x3.00); Sb (1,40.00); Cm (24:43)

TOF MS ES+
1.20e4



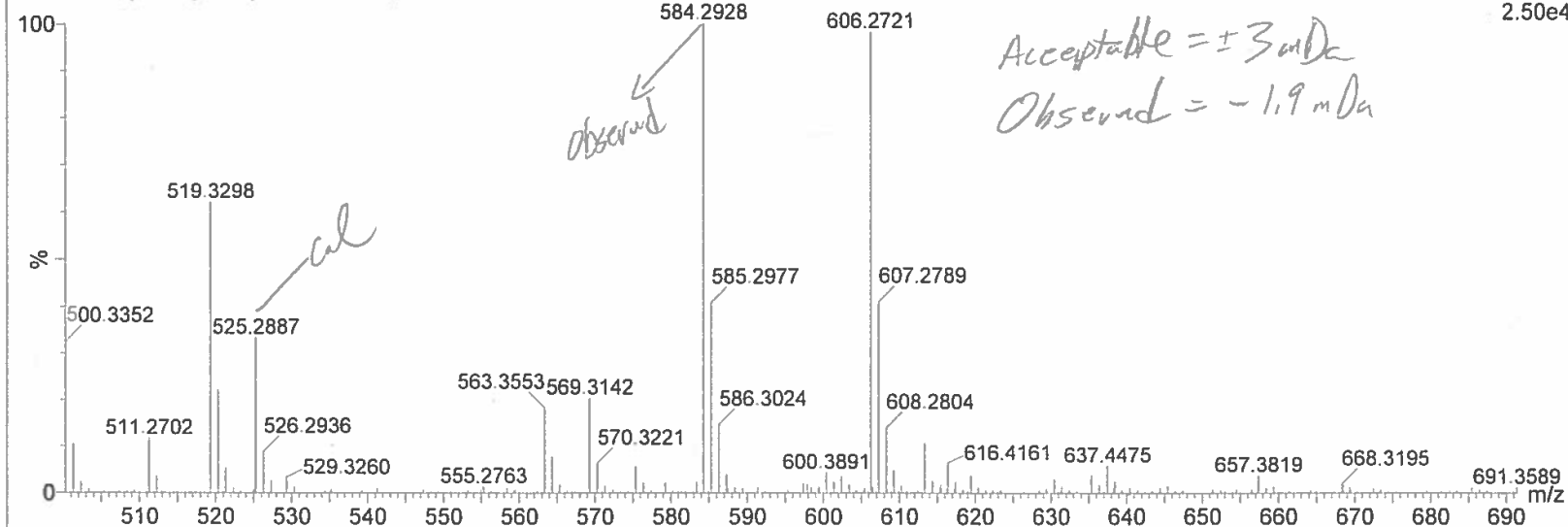
4129_a (0.019) ls (1.00,0.01) C₃₅H₄₂N₃O₃S

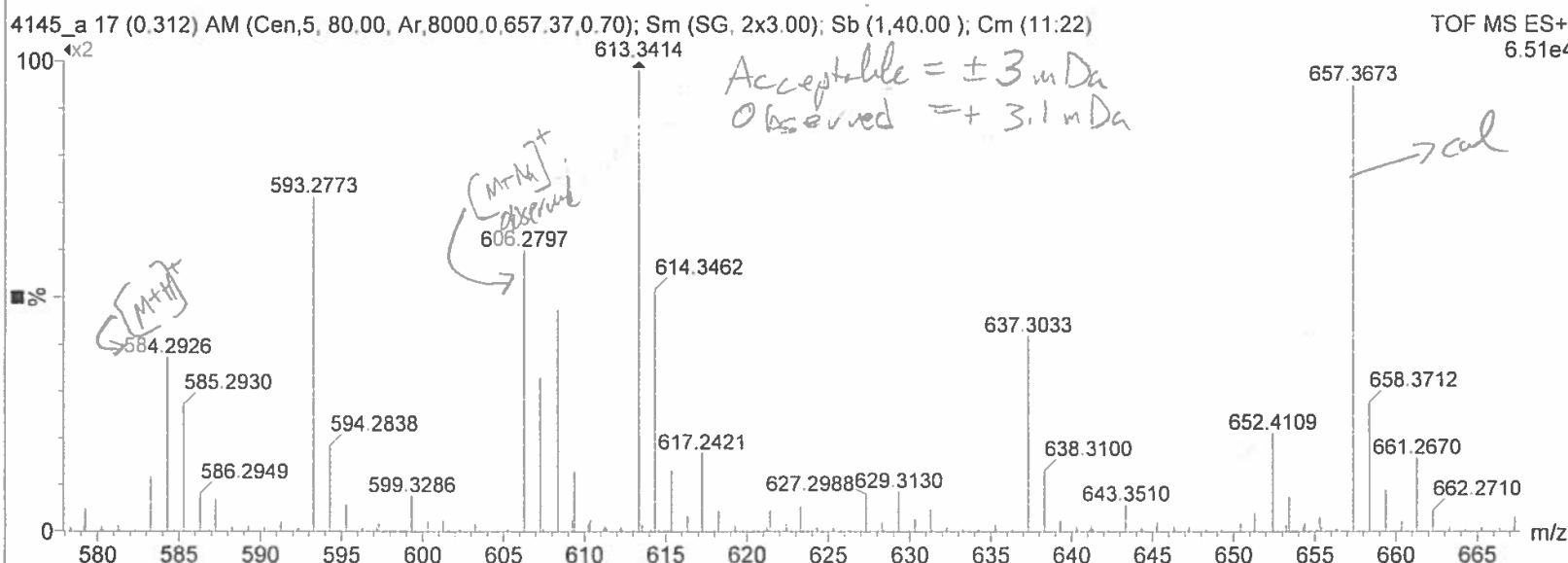
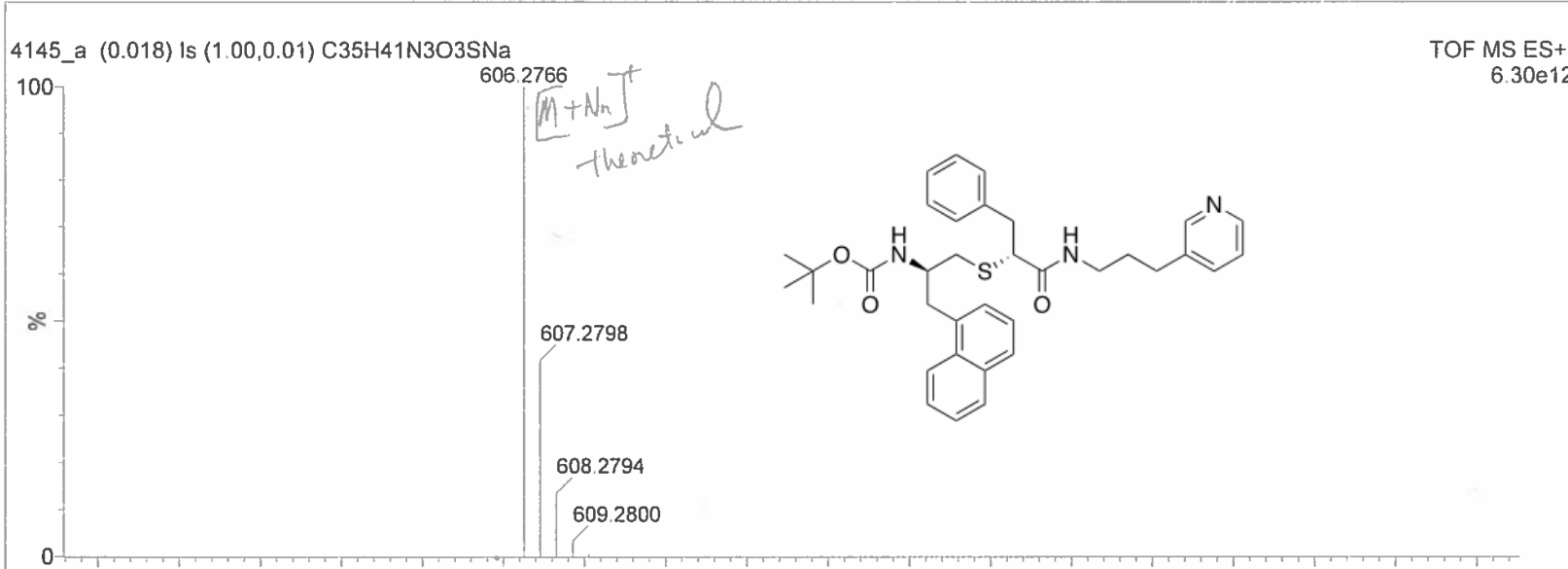
TOF MS ES+
6.30e12



4129_a 20 (0.367) AM (Cen,5, 80.00, Ar,8000.0,525.29,0.70); Sm (SG, 2x3.00); Sb (1,40.00); Cm (20:39)

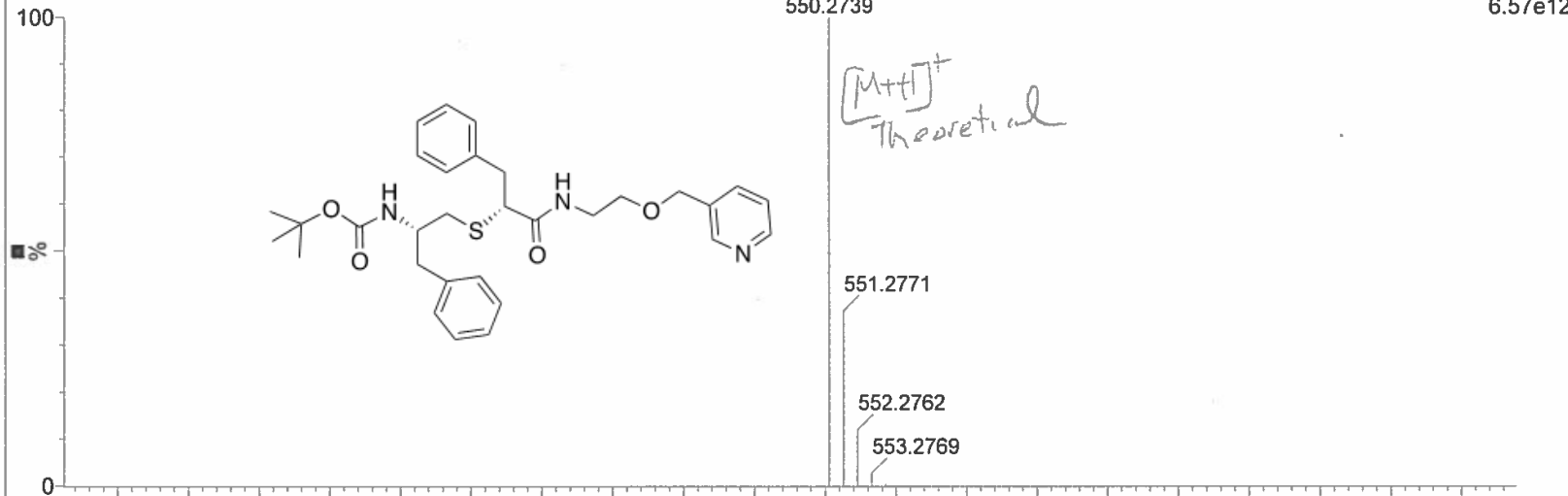
TOF MS ES+
2.50e4





4102_a (0.019) ls (1.00,0.01) C₃₁H₄₀N₃O₄S

TOF MS ES+
6.57e12



4102_a 17 (0.312) AM (Cen,5, 80.00, Ar,8000.0,525.29,0.70); Sm (SG, 2x3.00); Sb (1,40.00); Cm (11:26)

TOF MS ES+
1.76e4

